ANNUAL REVIEWS

Annual Review of Nuclear and Particle Science

High-Energy Extragalactic Neutrino Astrophysics

Naoko Kurahashi,[1] Kohta Murase,[2,3] and Marcos Santander[4]

[1]Department of Physics, Drexel University, Philadelphia, Pennsylvania, USA

[2]Department of Physics, Department of Astronomy & Astrophysics, Institute for Gravitation and the Cosmos, The Pennsylvania State University, University Park, Pennsylvania, USA

[3]Center for Gravitational Physics, Yukawa Institute for Theoretical Physics, Kyoto, Japan

[4]Department of Physics and Astronomy, University of Alabama, Tuscaloosa, Alabama, USA; email: jmsantander@ua.edu

Annu. Rev. Nucl. Part. Sci. 2022. 72:365–87

First published as a Review in Advance on July 18, 2022

The *Annual Review of Nuclear and Particle Science* is online at nucl.annualreviews.org

https://doi.org/10.1146/annurev-nucl-011122-061547

Keywords

neutrino astronomy, cosmic rays, extragalactic sources, galaxies

Abstract

The detection of an astrophysical flux of neutrinos in the TeV–PeV energy range by the IceCube Neutrino Observatory has opened new possibilities for the study of extreme cosmic accelerators. The apparent isotropy of the neutrino arrival directions favors an extragalactic origin for this flux, potentially created by a large population of distant sources. Recent evidence for the detection of neutrino emission from extragalactic sources includes the active galaxies TXS 0506+056 and NGC 1068. We here review the current status of the search for the sources of the high-energy neutrino flux, concentrating on its extragalactic contribution. We discuss the implications of these observations for multimessenger studies of cosmic sources and present an outlook for how additional observations by current and future instruments will help address fundamental questions in the emerging field of high-energy neutrino astronomy.

Contents

1. INTRODUCTION

Neutrinos are a unique probe of the high-energy cosmos. Their small interaction cross sections allow them to escape the dense regions of astrophysical sources that may be opaque to photons, and their paths are unaffected by intervening electromagnetic (EM) fields as they are electrically neutral. Neutrinos have been used as astrophysical messengers for decades, including the detection of MeV neutrinos from the Sun (1, 2) and supernova 1987A (3, 4).

At higher energies, in the GeV–TeV range and above, astrophysical neutrinos are expected to be produced in the interactions of hadronic particles, either at their acceleration site or during propagation through interstellar or intergalactic space. Neutrinos may therefore trace astrophysical particle acceleration sites and provide the solution to the cosmic-ray origin mystery. The discovery of an astrophysical neutrino flux in the 10-TeV to 10-PeV range (5) represents a breakthrough toward enabling high-energy neutrino astronomy. With no strong anisotropy observed in the arrival direction of these astrophysical neutrinos, especially lacking any directional signature that follows the Galactic Plane, it is likely that this flux is dominated by extragalactic sources. The observation of the high-energy diffuse flux combined with the tantalizing evidence for neutrino emission from the active galaxies TXS 0506+056 and NGC 1068 has put us at the doorstep of extragalactic neutrino astronomy.

We review here recent results from the study of high-energy astrophysical neutrinos and the implications for the sources of this flux, in particular the potential extragalactic contribution. We describe the current experimental landscape, introduce the detectors coming online in the near future, and discuss the connection between the neutrino observations and those in a broader multimessenger context involving photons, cosmic rays, and gravitational waves (GWs).

For the purposes of this review, we define high-energy neutrinos as those with energies starting in the GeV–TeV range and above. The reader is referred to recent reviews on the detection of

MeV neutrinos from the Sun (6) and from supernovae (7, 8) that gave birth to neutrino astronomy as a field.

2. NEUTRINO OBSERVATORIES, PRESENT AND FUTURE

The extremely small interaction cross sections [$\sigma_{\nu p} \sim 10^{-38}\,(E_\nu/\mathrm{GeV})\,\mathrm{cm}^2$] of neutrinos present a challenge to their detection upon arrival at Earth. Therefore, neutrino detectors have historically been large. As the neutrino energy increases, so does its cross section, but celestial neutrino emissions follow steeply falling power laws for which the rising cross section cannot compensate. The end result is a larger detector to target higher-energy neutrinos. Early estimates of the astrophysical neutrino flux level in the TeV–PeV energy range pointed to the necessity of a kilometer-scale neutrino detector, which would require a naturally occurring detection medium to make its construction economically feasible.

Current high-energy neutrino detectors implement the water Cherenkov technique originally proposed in 1960 by Markov (9) and independently by Reines (10) and Greisen (11). In this approach, a large natural body of water such as a deep lake, sea, or glacial ice is instrumented with a volumetric array of light sensors such as photomultiplier tubes (PMTs). These PMTs detect the Cherenkov photons emitted by relativistic charged particles produced in neutrino interactions, which allow the energy, direction, and flavor of the neutrino to be inferred. The first proposal for a kilometer-scale neutrino detector instrumented with PMTs was put forward by the DUMAND Collaboration (12), followed by the parallel development of the Baikal, AMANDA, and ANTARES instruments. The history of the pioneering efforts to make high-energy neutrino astronomy possible is recounted in Reference 13.

The two fully commissioned neutrino telescopes currently in operation are ANTARES and IceCube (**Figure 1**). ANTARES (14) has been operating in its final configuration since 2008 with 885 PMTs instrumenting a volume of about 0.01 km^3 of the Mediterranean Sea off the coast of Marseille, France. ANTARES will be superseded by KM3NeT (15), a neutrino telescope with two main components: ORCA, dedicated to the study of neutrino properties, and ARCA, optimized for high-energy neutrino astrophysics. In its final configuration, ARCA will consist of two blocks, each with 115 detector units (called strings) with 18 optical modules per string, which collectively will instrument a volume of $\sim$1 km^3. As of 2021, six detector units were operational in the ORCA site (off the coast of Toulon, France), and six were operational at the ARCA site near Portopalo di Capo Passero, Sicily, Italy (16).

The Baikal-GVD (Gigaton Volume Detector) (18) is a current effort to build a cubic-kilometer-scale detector in Lake Baikal, Russia, following the operation of previous detectors at the site. The detector consists of clusters of 288 PMTs arranged along eight strings each. The first phase, GVD-1, was deployed in 2021 and consists of eight clusters with 2,304 PMTs covering a volume of 0.4 km^3 (19).

IceCube (20, 21), deployed in the deep Antarctic ice near the South Pole, is the most sensitive high-energy neutrino telescope currently in operation and the first to reach the cubic-kilometer scale. The detector was completed in 2010 and consists of 5,160 PMTs distributed over 86 strings. The IceCube Neutrino Observatory includes IceTop (22), an air-shower array on the ice surface for cosmic-ray studies, and DeepCore, a denser, deeper array with improved sensitivity to neutrinos with energies down to 10 GeV (23). Most of the results discussed in this review come from IceCube, the preeminent neutrino observatory of the current generation.

The capability of these detectors to determine the energy, incoming direction, and flavor of the incoming neutrinos relies on the physics of weak interactions and the energy losses of the secondary particles they produce. Neutrinos and antineutrinos are almost always indistinguishable,

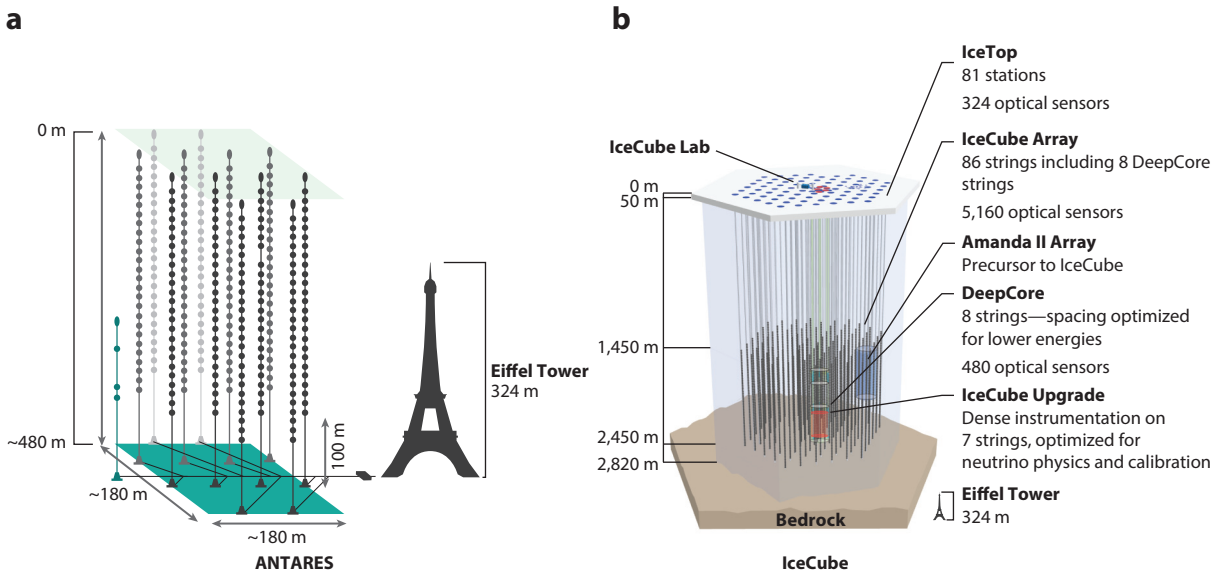

Figure 1

The current generation of high-energy neutrino telescopes: (*a*) ANTARES and (*b*) IceCube. The Eiffel Tower is shown for scale next to each detector as their scale is different. Panel *a* adapted from Reference 14 with permission from Elsevier. Panel b adapted with permission from Reference 17; copyright 2011 by the American Physical Society.

and in this discussion they are interchangeable. In the TeV range and above, neutrino interactions are dominated by deep inelastic scatterings between the incoming neutrino and quarks in the nucleon of the detection medium (24). Charged-current (CC) interactions mediated by the exchange of a $W^{\pm}$ boson result in a particle shower accompanied by a charged lepton with the same flavor as the incoming neutrino (i.e., $\nu_\ell + N \rightarrow \ell^- + X$). In a neutral-current (NC) interaction, $\nu_\ell + N \rightarrow \nu_\ell + X$, a particle shower is produced as the neutrino transfers a fraction of its energy to the nucleon via the exchange of a Z^0 boson. An additional channel is associated with the resonant production of W^- in $\bar{\nu}_e e^-$ interactions, the Glashow resonance (25), which dominates over neutrino–nucleon interactions at a neutrino energy of 6.3 PeV.

The main tool for high-energy neutrino astronomy is the detection of $\nu_\mu + \bar{\nu}_\mu$ via CC interactions. The low energy-loss rate of muons, with a longer lifetime compared with taus, allows them to travel for kilometers in water or ice while emitting Cherenkov photons (26). This has a twofold effect: It increases the effective size of the detector, which is now sensitive to muons from neutrinos interacting outside the instrumented volume, and it provides good angular resolution as the long muon tracks provide a long lever arm for muon directional reconstructions. The kinematic opening angle between the muon and the incoming neutrino is approximately $0.7° \times (E_\nu/1\,\text{TeV})^{-0.7}$ (27), which is typically smaller than the uncertainty introduced by our incomplete knowledge of light propagation in the natural detection medium. Therefore, both are considered collinear. The muon directional-reconstruction capabilities of current detectors have been validated through the study of the cosmic-ray Moon shadow (5, 28), which delivers a typical angular resolution $\lesssim 1°$. For comparison, events resulting from NC interactions and CC interactions of ν_e and ν_τ have angular resolutions of 5° to 15° (29, 30). These events, called cascades, are neutrino-induced showers that are <10 m—smaller than the string spacing of the detector—and combined with short scattering lengths of light, they look like cascades of photons emitted from a single point in the detector.

The search for astrophysical neutrinos is conducted in a background-dominated regime, where the main backgrounds are muons and neutrinos from cosmic-ray interactions in the atmosphere. These backgrounds have distinctive spectral, directional, and flavor characteristics that allow their separation from a putative astrophysical signal. In the sky above the horizon (zenith angle $\theta < 90°$), down-going muons represent the main background, although their soft spectrum above a few hundred GeV (asymptotically approaching $\propto E_\nu^{-3.7}$) limits their energies to $\lesssim$100 TeV. Atmospheric neutrinos can be detected over 4π sr, with conventional, mostly muon, neutrinos being produced in pion and kaon decays with a soft spectrum $\propto E_\nu^{-3.7}$ (31). The much-subdominant decay of charmed $D^\pm$ mesons introduces a predicted (32), but yet undetected, prompt neutrino background with a harder spectrum $\propto E_\nu^{-2.7}$ at $E_\nu \sim 100$ TeV and equal electron and muon neutrino contributions. By contrast, an astrophysical neutrino flux is expected to be in near equipartition of neutrino flavors, as they oscillate during propagation over very long distances (33).

3. DIFFUSE EMISSION

3.1. Diffuse Neutrino Observations

The most significant breakthrough in the last decade for extragalactic neutrinos is their actual observation. While they had been long hypothesized, the first observation of celestial emission of neutrinos in the TeV–PeV range occurred in 2013. The identification of PeV-energy neutrinos by IceCube (34), which were incompatible with the soft atmospheric neutrino background with 2.8σ, led to the development of an analysis targeting high-energy events with their interaction vertex contained within the IceCube instrumented volume. By defining a veto region in the outer parts of the detector, atmospheric muon and neutrino backgrounds were suppressed to a handful per year (35), uncovering the astrophysical spectrum at the highest-energy tail. While muon neutrinos interacting outside the detector have the advantage of higher statistical power, they were selected against in the discovery analysis (5) because of the high background expected in that sample. The resulting data set is dominated by cascade events that have superior energy resolution at 10–20% as the light deposition is contained in the detector. Despite the limited angular resolution of the sample, a search for point sources was performed and yielded no statistically significant evidence of directional clustering. In fact, the all-sky nature of the arrival direction along with a hard energy spectrum (best-fit flux was $\propto E_\nu^{-2.2}$) indicates that extragalactic neutrino flux dominates this diffuse emission.

The statistical significance of the initial discovery (for which the neutrino spectrum is shown in **Figure 2**) was 4.8σ—equivalent to a chance probability of 2×10^{-6} for background fluctuations causing such observations. Since then, the significance of the detection has increased as IceCube accumulates statistics, and the signal has also been observed in multiple analysis channels. The diffuse astrophysical neutrino flux is typically characterized using a power law of the form $\Phi_\nu(E_\nu) = \Phi_0(E_\nu/E_0)^{-\gamma}$, where the parameters are the spectral index γ and the flux normalization Φ_0 quoted at the normalization neutrino energy E_0. The flux can be quoted as per-flavor or all flavors combined assuming a 1:1:1 flux ratio among the three flavors (with $\nu + \bar{\nu}$ combined), and usually normalized at $E_0 = 100$ TeV. Fermi shock acceleration of cosmic rays typically predicts the flux of neutrinos to follow a power law with $\gamma = 2$ (36). Most astrophysical objects are, however, expected to have more complex neutrino emission profiles with an energy-dependent spectral index. Nonetheless, with statistical limitations of observations—and because an all-sky diffuse flux, which undoubtedly is the sum of many astrophysical source emissions, is being characterized as one flux—a single power-law fit remains the first test in characterizing the diffuse astrophysical neutrino flux.

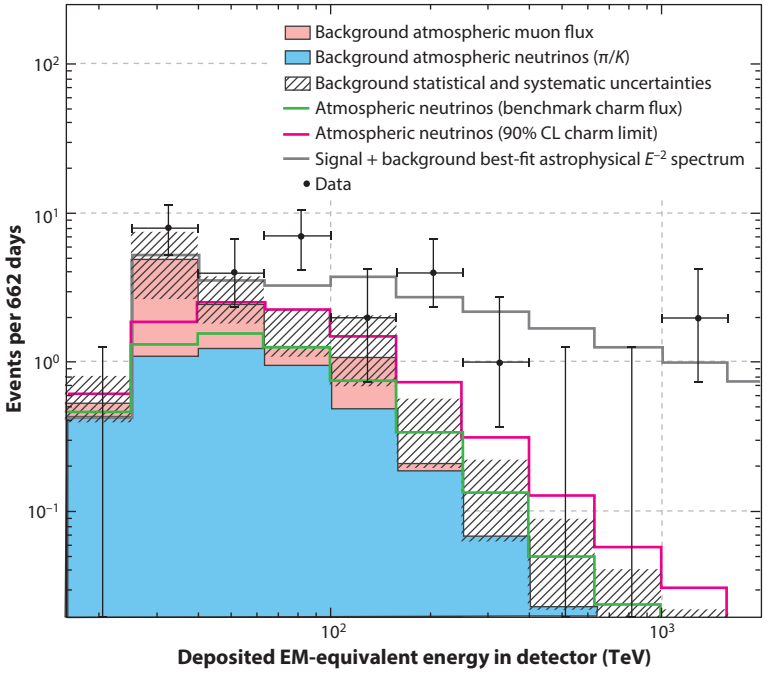

Figure 2

Distributions of the deposited energies of the observed events in the IceCube detector compared with model predictions, from the 2013 discovery paper (5). Figure adapted from Reference 5 with permission from AAAS. Abbreviations: CL, confidence level; EM, electromagnetic.

The discovery analysis used 2 years of IceCube data. Since then, this analysis channel has been updated a few times; the most recent analysis used 7.5 years of data (37). Another approach is to select for all tracks, not just ones originating within the detector. The track events analysis uses 9.5 years of IceCube events exclusively from the northern sky, thus suppressing astrophysical muons, and most effectively probes energy scales of hundreds of TeV. Finally, using shower events exclusively suppresses astrophysical muons almost completely and thus makes it possible to push the target energies lower. This analysis uses 6 years of all-sky IceCube events and most effectively probes tens of TeV. These results are summarized in **Table 1**. Differences between these observations can be due to many factors. The astrophysical diffuse flux may have different characteristics at different energy ranges, and the four analyses probe different source components. The flux is likely to vary depending on the part of the sky observed, and the muon neutrino analysis uses events only from the northern sky, whereas the others see the whole sky. The flux characterization

Table 1 Diffuse flux summary

Analysis	γ	Φ_0 at 100 TeV
Discovery updated (37)	2.87 ± 0.20	$6.37^{+1.47}_{-1.62}$
Upgoing tracks (38)	2.37 ± 0.09	$4.32^{+0.75}_{-0.78}$
Showers (39)	2.53 ± 0.07	$4.98^{+0.75}_{-0.81}$

Best-fit single power-law flux parameters of various diffuse flux analysis channels. Values are for an all-flavor combined flux assuming a 1:1:1 flavor ratio, neutrino and antineutrino combined, where Φ_0 is the flux normalization at 100 TeV in units of 10^{-18} GeV^{-1} cm^{-2} s^{-1} sr^{-1}.

may also depend on the neutrino flavor. Different neutrino production mechanisms at astrophysical sources lead to different neutrino flavor compositions. Neutrino oscillations over cosmological distances will push toward an even flavor ratio but perhaps not completely.

3.2. Multimessenger Connection

One of the most important conclusions from the IceCube observation of high-energy neutrinos is that the diffuse neutrino flux in the range of 0.1 to 1 PeV is comparable to those of the diffuse γ-ray background flux in the sub-TeV range (40) and the ultrahigh-energy cosmic-ray (UHECR; $E \gtrsim 10^{18.5}$ eV) flux. This implies that the energy generation rate densities of high-energy neutrinos, high-energy γ-rays, and UHECRs are all comparable to $\sim 10^{44}$–10^{45} erg Mpc^{-3} y^{-1} (41). This gives profound constraints on the candidate sources of high-energy neutrinos and may indicate the possible connection among three cosmic particle channels (42, 43). For grand unified scenarios, which aim to simultaneously explain the diffuse fluxes of all three messengers, cosmic-ray reservoirs are among the most promising candidate source classes (44).

The neutrino and γ-ray connection (**Figure 3**) is unavoidable because neutrinos should be accompanied by hadronic γ-rays. Murase et al. (44) confronted the IceCube data above 0.1 PeV with the isotropic diffuse γ-ray background measured by *Fermi* and placed constraints on the dominant sources of high-energy cosmic neutrinos. In particular, if the neutrinos are produced by

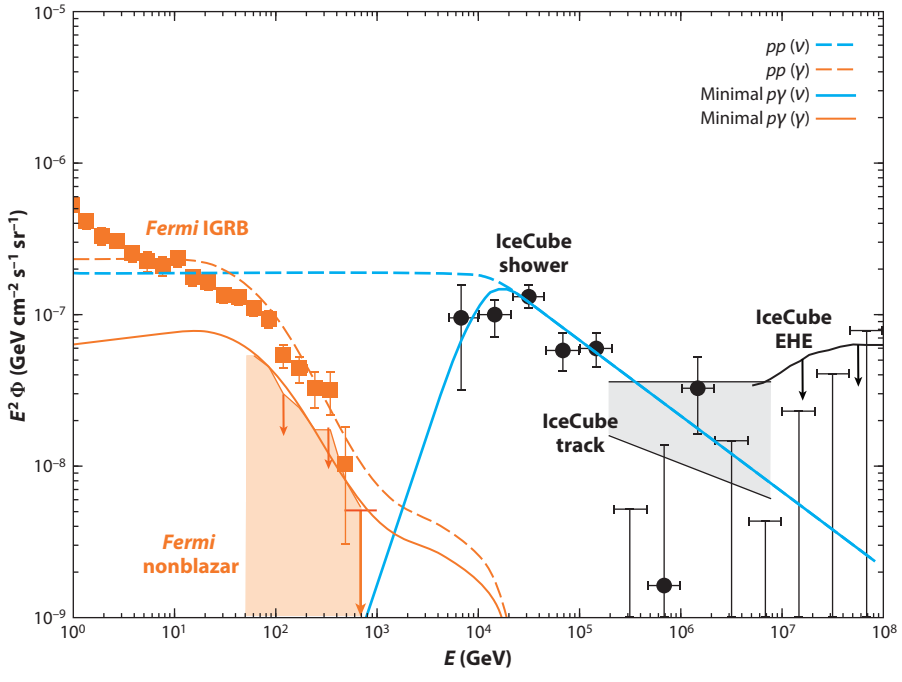

Figure 3

Neutrino and γ-ray connection of all-sky neutrino (39, 49, 50) and γ-ray fluxes (40). For generic models to explain the IceCube data in the range of 10 to 100 TeV, whether neutrinos are produced via a *pp* or $p\gamma$ process, γ-rays associated with neutrinos violate the nonblazar component of the extragalactic γ-ray background measured by *Fermi*. Figure adapted with permission from Reference 46; copyright 2016 by the American Physical Society. Abbreviations: EHE, extremely high energy; IGRB, isotropic diffuse γ-ray background.

pp interactions and the sources are transparent to γ-rays, the spectral index is constrained to be $\gamma \lesssim 2.1$–2.2. This also implies that a steep spectrum of the diffuse neutrino flux cannot be readily reconciled with the diffuse γ-ray flux seen by *Fermi*. Indeed, the latest shower data in the range of 10 to 100 TeV have deepened the mystery about the origin of high-energy cosmic neutrinos (39). Detailed multimessenger analyses indicate that the hadronic γ-ray flux associated with the diffuse neutrino flux in the range of 10 to 100 TeV violates the nonblazar (nonpoint source) contribution of the diffuse γ-ray flux (45). This suggests the existence of a class of high-energy neutrino sources that are opaque for GeV–TeV γ-rays, which can be naturally realized if neutrinos are produced by $p\gamma$ interactions (46–48).

4. EXTRAGALACTIC SOURCES: EXPERIMENTAL RESULTS

In this section, we highlight significant experimental results of the last decade in searching for extragalactic sources of neutrino emission.

Searches for correlations between neutrino data and known sources can take place by analyzing source positions one at a time or by stacking sources that belong to the same catalog class to look for correlations simultaneously. The first method provides clear answers on whether individual sources are responsible for high-energy neutrino emission, but statistical trials must be taken into account for the look-elsewhere effect, which can weaken the statistical significance of observations if many sources are considered. Each collaboration keeps a list of potential neutrino sources (51–53) with individual selection criteria based on EM observations, mostly from *Fermi*-LAT and TeV source catalogs [e.g., 4FGL (54), 3LAC (55), TeVCat (56)]. Active galactic nuclei (AGNs) belonging to different subclasses, such as BL Lacertae objects and flat spectrum radio quasars (FSRQs), dominate this list. The stacking method looks at a class of sources together and therefore would be the first to see a signal if several weak sources emerged. However, this type of analysis is sensitive to the relative weighting of the fluxes assumed in the search. For example, weighting all sources in a catalog equally provides very different outcomes in most stacking analyses compared with, say, weighting them by their γ-ray flux (i.e., assuming that the neutrino flux of each source in the catalog scales proportionally to its observed γ-ray flux). Thus, stacking analyses answer hypotheses not only about a particular class of sources being neutrino emitters but also about the specific relative neutrino fluxes emitted.

Another way to divide these analyses is between time-dependent and time-integrated searches. Some searches, such as searches of neutrinos coincident with γ-ray bursts (GRBs), naturally have a time dependence in the analysis. An external event triggers a search window in time. Other sources that are known to continuously emit γ-rays would be searched for neutrinos in a time-integrated way aiming to accumulate enough data so that the neutrino signal would surpass the background expectations. Much like the time-integrated analyses, these bursts or flares can be searched individually (taking into account trials) or stacked, as described in the paragraph above.

Finally, an inherently multimessenger approach is to issue neutrino alerts of significant events (57, 58) or to receive alerts from other observatories to follow up on neutrinos in real time (59–61). In this approach, as described in Section 6, neutrino signals are correlated in space and time with photons or GWs, improving the sensitivity to joint emitters of these messengers. Additionally, full-sky scans of neutrino hotspots are performed to search for sources without any assumptions of counterparts. This can be done by time-integrated hotspot searches (29, 51–53, 62) and untriggered flare searches (63).

Correlation searches between neutrino observations and known extragalactic sources have been performed for several decades (64). However, to date, only two sources have emerged as tantalizing neutrino sources: the active galaxies TXS 0506+056 and NGC 1068.

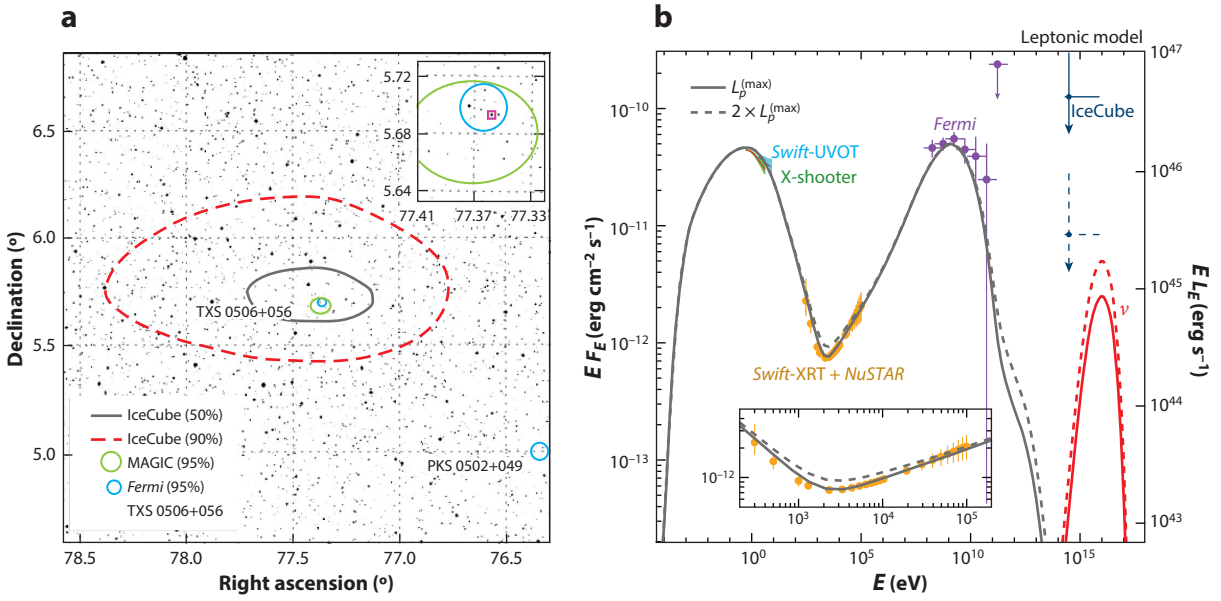

Figure 4

(*a*) Position of IceCube-170922A with angular uncertainties and TXS 0506+056. Panel adapted from Reference 68 with permission from AAAS. (*b*) Multimessenger spectra of TXS 0506+056. All-flavor neutrino flux upper limits are shown for 0.5 years (*solid blue line*) and 7.5 years (*dashed blue line*). Panel adapted from Reference 110 with permission from AAS.

4.1. Blazars

The IceCube Neutrino Observatory issues real-time alerts to the astronomical community when high-energy neutrino events of likely astrophysical origin are recorded in the detector (65). On September 22, 2017, such an alert (66) was issued upon the detection of a neutrino event, IceCube-170922A. The position of the event was found to be coincident in time and direction with the γ-ray blazar TXS 0506+056, as shown in **Figure 4*a***, which at the time was flaring in γ-rays and X-rays. Further investigation of IceCube archival data from this location found evidence of a neutrino flare from September 2014 to March 2015. The coincidence of such a neutrino alert event arriving from a flaring source in *Fermi*-LAT constituted 3σ evidence for neutrino emission from the direction of TXS 0506+056 (67). Independently, the neutrino flare of 2014–2015 represents a 3.5σ observation (68). This was the first compelling evidence of any high-energy neutrino source in the history of multimessenger astronomy.

Blazars have been studied using a stacking approach (69–73), but correlations have not been observed, even when TXS 0506+056 is present in the catalog since it becomes one of many sources considered simultaneously. When neutrino flares are searched over the entire sky (63), the 2014–2015 flare becomes statistically insignificant because of the look-elsewhere effect. This highlights the advantage that neutrino source searches gain by having an external trigger from another messenger that singles out a source of interest.

4.2. Other Types of Active Galactic Nuclei

By 2018, IceCube had observed an excess in their source list search at the location of the Seyfert II galaxy NGC 1068 (51) at the 2.9σ level. This source was also within the extended region of the most significant hotspot in the Northern Hemisphere in the full-sky scan, as shown in

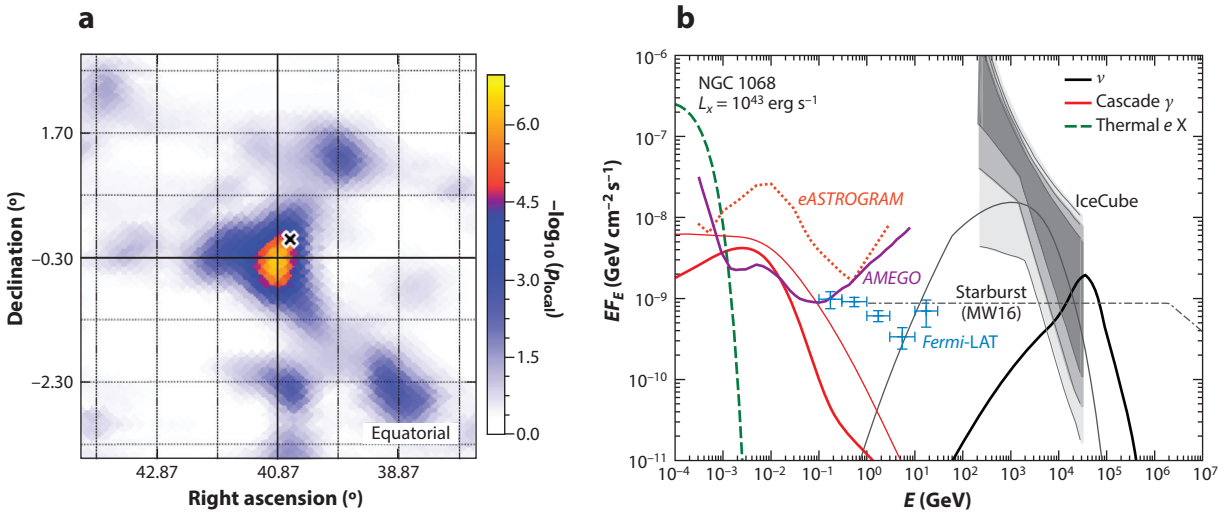

Figure 5

(*a*) Significance map of high-energy neutrinos. The position of NGC 1068 is indicated by the cross. Panel adapted with permission from Reference 51; copyright 2020 by the American Physical Society. (*b*) Multimessenger spectra of NGC 1068. Black curves represent neutrinos, and red curves represent γ-rays. Thick curves correspond to a model for NGC 1068 while thin curves are for a model explaining the all-sky neutrino flux. Panel adapted from Reference 130; copyright 2020 by the American Physical Society.

Figure 5*a*. This was the first time that a time-integrated search had resulted in a hotspot at this level of statistical significance. NGC 1068, at a distance of ∼14 Mpc, is the most luminous Seyfert II galaxy detected by *Fermi*-LAT, making it an unsurprising source to emerge this way. The analysis used 10 years of IceCube data, illustrating that cumulative long-term neutrino data can deliver evidence of sources, in addition to time-domain search techniques such as those used to identify TXS 0506+056. As more data accumulate, stronger evidence of more sources is likely to emerge.

Perhaps comfortingly, another location that emerges as a hotspot in the IceCube full-sky scan of 10 years of time-integrated data is TXS 0506+056. The data used here encompass the alert event IceCube-170922A and the 2014–2015 flare period. An assessment of how the time-integrated significance grows compared with the time-dependent behavior of neutrinos from sources will become increasingly interesting for many sources.

4.3. Gamma-Ray Bursts and Other Transients

Before neutrino telescopes were operational at their current large scales, the most favorable sources were considered to be GRBs. However, by 2012, IceCube had established an absence of energetic neutrinos associated with GRBs (74), but the limits were still consistent with the standard theoretical predictions (75–77). GRBs are stacked in time and position or analyzed individually to search for coincident neutrinos, where neutrinos are analyzed to come on time or with a time shift. The well-localized nature of GRBs in time and position gives neutrino analyses a nearly background-free opportunity to search for coincident neutrinos. Despite this highly favorable search condition and continuous improvements in analysis sensitivities, no correlations have been found (78–84), which may point to more conservative predictions or other models predicting lower-energy neutrino emission (85).

Supernovae, which were established as MeV neutrino emitters, are also promising sources of high-energy neutrinos. Not only follow-up searches (86) but also stacking searches (87–89) have been performed for broadline type Ibc and type IIn supernovae, but no significant excess has been found.

Tidal disruption events (TDEs), where a star is ripped apart by tidal forces in the vicinity of a supermassive black hole, have recently been suggested to correlate with neutrino emission (90) due to a neutrino alert event in the vicinity of a very bright TDE. Previous stacking analysis of multiple TDEs from IceCube (91), however, did not observe a correlation of statistical significance, nor did a time-integrated search of TDEs from ANTARES (92).

4.4. Sources of Other Messengers

GW alerts are followed up by neutrino telescopes to search for coincident neutrinos. The famous multimessenger detection of the event GW170817 associated with a GRB and a kilonova/macronova was followed up by neutrino telescopes (93–95). Other GW events—GW170104 (96), GW15226 (97), and GW150914 (98)—were also analyzed in searches for neutrino counterparts, as well as entire runs of LIGO and Virgo (99–102). No associated neutrino emission was identified in these searches, and upper limits on the neutrino luminosity of these events were derived.

UHECRs can also be correlated with neutrinos under the assumption that their arrival directions are not completely scattered during propagation by Galactic and intergalactic magnetic fields. As UHECRs interact with ambient photons and matter at their acceleration sites or during propagation, the neutrino emission may trace the positions of their sources, which could be revealed in a joint analysis (103, 104). No correlation between UHECRs and neutrinos has been identified so far.

As both GW and UHECR correlation studies have yielded null results, photons remain the only other messenger for which evidence of a neutrino correlation is observed.

5. EXTRAGALACTIC SOURCES: CANDIDATES

5.1. Active Galactic Nuclei

AGNs are among the most promising candidate sources of high-energy cosmic rays and neutrinos. They typically host supermassive black holes with masses of $\sim 10^6$ to $10^9 M_\odot$, and the accretion onto the black hole powers radiation from the accretion disk and its coronae as well as winds. The black holes are believed to rapidly spin, which also drives powerful relativistic jets.

5.1.1. Blazars and TXS 0506+056. AGNs with powerful jets may point to the Earth; these are called blazars. Their emission is strongly beamed and nonthermal, and the spectral energy distributions are composed of two humps. The low-energy hump is attributed to synchrotron emission from electrons accelerated in the jet, while the origin of the high-energy hump has been debated. In the leptonic scenario, γ-rays are explained as inverse Compton emission. In the hadronic scenario, cosmic-ray-induced cascade emission (105) and/or cosmic-ray synchrotron emission (106, 107) are responsible for the observed γ-rays. In either scenario, not only electrons but also ions are accelerated, and lepto-hadronic models have been widely investigated.

Accelerated ions produce neutrinos through pp and $p\gamma$ interactions, and the latter process is typically more important in blazars. For BL Lacertae objects, target photons are mainly synchrotron photons from relativistic electrons that are coaccelerated together with ions. External radiation fields, which can be broadline emission in the ultraviolet range, dust emission at the infrared band, and scattered disk–corona emission in the ultraviolet and X-ray range, play dominant roles in neutrino emission from FSRQs. The neutrino spectrum is predicted to be

hard if the cosmic-ray spectrum follows $\propto E^{-2}$ or somewhat steeper. Blazars are typically EeV neutrino emitters if these are the sources of UHECRs (for a review, see, e.g., Reference 108), and the limits on extremely high-energy ($E_\nu \gtrsim 10$ PeV) neutrinos (50) have placed important constraints on the models.

TXS 0506+056 is a blazar with an intermediate luminosity, which may be classified between a BL Lacertae and an FSRQ, although it may be a masquerade blazar (109). Detailed numeric modeling based on a single emission zone model suggests that it is challenging to build a concordance picture of multimessenger emission from the optical, X-ray, and γ-ray bands as well as neutrinos. For the 2017 multimessenger flare, the *Swift* and *NuSTAR* X-ray data clearly show a valley in the spectrum, by which the neutrino and cosmic-ray luminosities are strongly constrained (see **Figure 4*b***). This is because γ-rays, electrons, and positrons associated with neutrinos inevitably initiate EM cascades with a broad spectrum over the wide energy range, which would fill the valley if the neutrino flux was as high as the upper limit (110–114). The interpretation is more challenging for the 2014–2015 neutrino flare, which did not show the coincident flare in either γ-rays or X-rays, and the EM cascade flux associated with the neutrino flux violates the X-ray and/or γ-ray data (115–118). Alternative models, which include the neutral beam model and two-zone models with the γ-ray hidden region, have been proposed to avoid the constraints from EM cascades (115, 119, 120). However, the situation is still controversial. Although a few more coincidences have been reported (121–125), further observations and theoretical investigations are necessary to establish blazars as the source of high-energy neutrinos.

5.1.2. Nonjetted active galactic nuclei and NGC 1068. Most AGNs are radio quiet without possessing powerful jets (although they may have weak jets that are often inferred by radio observations), and they are typically Seyfert galaxies and quasars. The vicinity of black holes has been discussed as a possible site of particle acceleration and resulting neutrino emission (126, 127). Historically, accretion shocks have been considered as possible particle acceleration sites (128), and the diffuse neutrino flux in this scenario has been calculated (129). However, the existence of accretion shocks is in question, and the model has been constrained by neutrino observations.

In the standard disk–corona picture, X-ray emission is attributed to Comptonized disk photons, where the high-temperature corona is expected to form around the disk through magnetic dissipation. The coronal region is magnetized and turbulent, where ion acceleration can occur through magnetic reconnections and stochastic acceleration. For magnetically powered coronae in Seyfert galaxies and quasars, high-energy neutrinos in the range of 10 to 100 TeV are predicted, which can account for the all-sky neutrino flux in this medium-energy range (130). Bethe–Heitler pair production is important as an energy loss process of cosmic rays, and MeV γ-rays are unavoidably generated through EM cascades.

The association of high-energy neutrinos with NGC 1068 is intriguing in several aspects (**Figure 5*b***). First, NGC 1068 is a starburst coexisting with an AGN. Second, NGC 1068 is a Compton-thick Seyfert galaxy, in which X-rays are largely absorbed. The IceCube observation of NGC 1068 is consistent with either an accretion shock or magnetically powered corona model (130–132). In the disk–corona model, NGC 1068 is predicted to be the brightest neutrino source in the northern sky, and the model can critically be tested by IceCube and IceCube-Gen2; a few brighter sources in the southern sky are also expected to be observed by KM3NeT and Baikal-GVD (133). Multimessenger observations are important as well, and in particular MeV γ-ray observations will serve as a complementary probe of particle acceleration in the vicinity of supermassive black holes.

5.2. Violent Transients

The high-energy sky is extremely dynamic, with violent astrophysical events occurring over very short timescales, down to a few seconds in the case of γ-ray bursts. The high EM luminosities of these events, combined with their capability to accelerate particles to very high energies, make them promising neutrino sources, and their short duration significantly reduces the atmospheric background against which an astrophysical signal may be identified.

5.2.1. Tidal disruption events. As a star is torn apart by a supermassive black hole causing a TDE, about half of its mass is unbound, while the other half is expected to accrete onto a black hole or go outward as winds. TDE thermal emission, which can be produced by accretion disks, interactions of tidal streams, and winds (through reprocessing), has been observed in the optical and X-ray bands. Some of the TDEs are believed to have powerful jets; Sw 1644+57 is an example of a powerful TDE with strong X-ray emission (134). Since then, jetted TDEs have been actively discussed as the sources of high-energy neutrinos (135–138). Nonjetted TDE neutrino emission has also been considered, where neutrinos may come from accretion disks, coronae, and subrelativistic outflows interacting with the TDE debris or clouds (139, 140).

AT 2019dsg was a luminous TDE and was associated with IceCube-191001A (90). The optical luminosity at the peak is $L_{\rm OUV} \sim 10^{44}$ erg s^{-1}, and the neutrino event was observed 150 days after the peak. This TDE was detected in the radio and X-ray bands and was accompanied by infrared echo emission. AT 2019fdr was another very luminous optical transient; it was associated with IceCube-200530A (141). The optical luminosity at the peak is $L_{\rm OUV} \sim 10^{45}$ erg s^{-1}, and the neutrino was seen 320 days after the peak. This TDE was also accompanied by a radio counterpart. These detections may hint at TDEs as one of the contributors to the all-sky neutrino flux.

5.2.2. Long gamma-ray bursts and supernovae. A massive star with a mass of $\gtrsim 8\ M_\odot$ ends its life with a violent explosion, which is a supernova. It is accompanied by emission of thermal neutrinos in the 10-MeV range, and a fraction of the released gravitational binding energy is transferred to the kinetic energy, which is typically $\sim 10^{51}$ erg. The ejecta typically expands with a high velocity of ~3,000 to 10,000 km s^{-1}, forming a strong shock, where the diffusive shock acceleration mechanism operates. Supernova remnants are believed to be primary candidate sources of Galactic cosmic rays, and they have been observed in γ-rays.

Supernovae are natural sources of optical photons that originate from radioactive nuclei, shock heating, and perhaps energy injection by the central engine. Recent optical surveys revealed that it is common for supernova progenitors to be accompanied by the massive eruption of circumstellar material or inflation of the stellar envelope. It has been suggested that such a system is a promising source of high-energy neutrinos (142–144). For ordinary type II supernovae, IceCube, KM3NeT, and Baikal-GVD may detect ~100–1,000 neutrinos in the TeV range, and even millions of sub-TeV neutrinos can be detected if Betelgeuse explodes (144). Type IIn supernovae are powered by collisions with their circumstellar medium, and neutrinos from nearby supernovae are detectable (142, 145). Detecting high-energy neutrinos is important to reveal ion acceleration in the early stages of supernovae and to reveal the origin of PeVatrons.

GRBs are among the brightest explosive phenomena in the universe. For long GRBs, their prompt emission lasts ~10–1,000 s and is believed to originate from relativistic jets that are launched by a black hole or magnetar. Ions can be accelerated by jets, and high-energy neutrinos can be produced mainly via $p\gamma$ interactions (146). The predicted fluxes have large uncertainties (76, 77, 147), and the current limits start to give stringent constraints on the models. In the classical scenario, prompt γ-ray emission is attributed to synchrotron radiation from relativistic electrons that are accelerated at internal shocks. However, recent observations

and theoretical studies led to alternative scenarios, such as photospheric emission and magnetic dissipation scenarios. In the photospheric emission scenario, GeV–TeV neutrinos may be more promising (148–150). This is because cosmic-ray acceleration via the diffusive shock acceleration mechanism is suppressed when the shocks are radiation mediated, although ions can still be accelerated through the neutron conversion.

Ions can be accelerated up to ultrahigh energies at the external reverse shock during the afterglow phase, in which EeV neutrinos can be produced (151–153). A significant fraction of GRBs have X-ray and ultraviolet flares, which may also dominate neutrino emission from GRBs (154, 155).

Low-luminosity GRBs and transrelativistic supernovae are regarded as intermediate objects between GRBs and supernovae, and they can be major sources of high-energy neutrinos and UHECRs (156–159). They are less luminous but more common. Recent studies have indicated that some supernovae are powered by jets and/or magnetar winds, which may also be promising sources of high-energy neutrinos and UHECRs (160–165). In particular, choked jets have been suggested as the source of the all-sky neutrino flux in the range of 10 to 100 TeV (160, 166).

5.2.3. Short gamma-ray bursts and compact binary mergers. Binary neutron star mergers, neutron star–black hole mergers, and binary black hole mergers, which are powerful sources of GWs, have been discussed as potential sources of high-energy neutrinos. In particular, double neutron star mergers are widely believed to be the progenitors of short GRBs, and the detection of GW170817 associated with GRB 170817A supported this hypothesis. High-energy neutrinos from short GRBs have been investigated mostly in light of the jet scenario (167–169), and neutrino emissions during the extended and plateau emission phases are likely to be dominant (167). High-energy neutrinos may also be produced in choked jets (170), as well as by winds from the remnant black hole or magnetar (171, 172). Black hole mergers could also be neutrino emitters if there is matter around the binaries (for a review, see, e.g., 85).

5.3. Cosmic-Ray Reservoirs

Magnetized environments, in which cosmic rays are confined, provide natural sites for the production of high-energy neutrinos and γ-rays. If cosmic-ray accelerators (e.g., supernovae, AGNs) are embedded in such environments, cosmic rays escaping from the accelerators may diffuse and cause pp and $p\gamma$ interactions. In extragalactic space, the most promising sources, which are regarded as cosmic-ray reservoirs, are galaxies and galaxy groups.

5.3.1. Galaxy clusters and groups. Galaxy clusters are known to have magnetic fields with a strength of $\sim$0.1 to 1 μG, which can confine cosmic rays over cosmological timescales. It has been suggested that galaxy clusters and groups are the sources of high-energy cosmic rays around the "second knee" at $\sim 10^{17}$ eV, a softening in the cosmic-ray spectrum, or even UHECRs. There are two potential acceleration sites. The first is shocks associated with large-scale structure formation, which involve accretion shocks and merger shocks. Second, cosmic rays may be accelerated by AGNs and/or supernovae that are embedded in clusters and groups. Low-energy cosmic rays are expected to lose their energies via adiabatic losses, while sufficiently high-energy cosmic rays above PeV energies can escape into the intracluster medium without significant energy losses. Interestingly, the IceCube data above 100 TeV are consistent with earlier theoretical predictions for neutrino emission from galaxy clusters and groups (173, 174). However, the accretion shock model, where cosmic rays are produced at accretion shocks around the virial radius, is already disfavored because of constraints from neutrino anisotropy and radio observations (42, 175, 176). In contrast, the AGN model is still viable, where cosmic rays are supplied by AGNs including

radio galaxies, and low-mass clusters at high redshifts make a significant contribution to the all-sky neutrino flux (44, 177).

The fact that the energy generation densities of three messenger particles are all comparable suggests that their sources may be physically connected. Indeed, galaxy clusters can trap cosmic rays, by which high-energy neutrinos below a few PeV can be explained with a hard spectrum (177, 178). The nonblazar component of the isotropic diffuse γ-ray background is also explained simultaneously, in which cosmogenic γ-rays give a significant contribution. High-energy cosmic rays above 100 PeV may escape, and it has been suggested that cosmic rays around the second knee may come from AGNs or galaxy clusters (173). The hard spectrum of UHECR nuclei can be reproduced through the magnetic confinement and photodisintegration during the escape from the intracluster medium.

5.3.2. Star-forming galaxies. Star-forming galaxies showing the most active star formation are often called starburst galaxies, and they typically have high column densities and strong magnetic fields with ∼0.1–1 mG. Cosmic rays supplied by supernovae or other transients related to massive stars can be confined for millions of years and produce neutrinos and γ-rays (179, 180). For galaxies like the Milky Way, the cosmic-ray diffusion is so effective that the cosmic-ray spectrum on Earth, $\propto E^{-2.7}$, is steeper than the injected spectrum. In starburst galaxies, the gas density is so high that cosmic rays can lose their energies via *pp* interactions or adiabatic cooling before they diffusively escape, where the spectrum of neutrinos and γ-rays can be as hard as the observed neutrino spectrum. For starburst galaxies to be a major contributor of IceCube neutrinos in the PeV range, cosmic rays need to be accelerated beyond 100-PeV energies. This could be achieved by hypernovae or other energetic transients, stronger magnetic fields, galactic winds, and AGNs embedded in highly star-forming galaxies (44, 181–184). Recent studies have shown that star-forming galaxies give a significant contribution to the isotropic diffuse γ-ray background (185, 186). However, their contribution to the all-sky neutrino flux is likely to be subdominant at least below 100 TeV, although they can still make a sizable contribution above 100 TeV given that the cosmic-ray spectrum is harder than $\propto E^{-2.2}$.

6. EXTRAGALACTIC NEUTRINOS AND THEIR MULTIMESSENGER SYNERGIES IN THE COMING DECADE

The coming decade holds the promise of fully enabling extragalactic neutrino astronomy thanks to significant advances in our observational capabilities. Efforts are currently underway that aim to increase the number, sensitivity, and energy reach of neutrino telescopes and to establish new multimessenger studies as additional EM and GW observatories come online.

6.1. Improving Neutrino Observations

As described in Section 4, detection of extragalactic neutrino sources via time-integrated analyses, such as the one that provided evidence for NGC 1068, is performed in a background-dominated regime but with high neutrino event rates. Enough data must accumulate before such a signal emerges. Associating individual neutrino events with extragalactic sources, as with real-time alerts, is also possible if the neutrino energy is sufficiently high ($\gtrapprox$100 TeV) as the atmospheric background becomes subdominant at those energies; such is the case with the association between TXS 0506+056 and the IceCube-170922A event. A cubic-kilometer telescope such as IceCube may detect only $\mathcal{O}(10)$ events per year across the entire sky for such individual-alert events. Both approaches are limited by how quickly detectors can accumulate high-energy events.

Other approaches rely on shower or cascade events. Their primary advantage is the absence of atmospheric muons and atmospheric muon neutrinos detected via CC interaction as

backgrounds. This makes them suitable for analyses of sources above the local horizon, where using track events would include atmospheric muon backgrounds many orders of magnitude above the neutrino signal. They are also suited for extended regions of neutrino emission, given their limited angular resolution, and for correlation studies with short EM transients as the background can be significantly reduced owing to the short duration of these events. The main limitation for cascade events is their angular resolution, which is limited by understanding the local optical properties of the detector media.

For neutrino astronomy, the main improvements to these searches therefore involve increasing data collection through the construction of additional neutrino telescopes (or the expansion of existing ones), improving the angular resolution of the detectors, and further integrating the neutrino telescopes with the multimessenger astronomy community to discover more correlations in near-real time.

The increase in high-energy event rates will be delivered by next-generation instruments such as IceCube-Gen2 (187), which aims to increase the instrumented volume of the current-generation IceCube to ~ 8 km^3. In 10 years of operation IceCube-Gen2 will reach a 5σ energy flux sensitivity of the order of 10^{-12} erg cm^{-2} s^{-1} in the range of 0.1 to 1 PeV, a similar level as that achieved at current very-high-energy (VHE) γ-ray observatories in the EM domain. Additional sensitivity will be provided by KM3NeT-ARCA (15), Baikal-GVD (18), and the recently proposed P-ONE telescope (188), which are expected to reach the cubic-kilometer scale in the coming decade. In the $E_\nu \gtrapprox 100$ TeV energy range, neutrino absorption in the Earth becomes significant, reducing the detector's effective areas to neutrinos passing through the Earth (i.e., upgoing in the horizontal coordinate frame of the detector). Because of the high muon background for downgoing neutrinos, and absorption effects for upgoing ones, the peak sensitivity for neutrino telescopes in this energy range is near the local horizon. For midlatitude detectors like KM3NeT and Baikal-GVD, this means that the region of maximum instantaneous sensitivity sweeps the sky as the Earth rotates, which is relevant for transient searches, while for IceCube and IceCube-Gen2 it will remain near the celestial equator. Given these instruments' different locations and different capabilities, searches for extragalactic neutrino sources may benefit from a joint effort that combines data from all neutrino telescopes (189).

Improvements in the angular resolution of neutrino telescopes will also enable more sensitive and critical searches for extragalactic sources (42), especially given their large number and the possibility of source confusion. The sensitivity of point-source searches scales roughly with the inverse of the point-spread-function radius of the instrument, while the probability of chance correlations for single events scales with the radius squared (i.e., it is proportional to the solid angle of the uncertainty region of the neutrino event). This means that even modest improvements in angular resolution could deliver significant sensitivity enhancements that are equivalent to longer exposure times for steady sources and could also prove vital in pinpointing neutrinos coincident with rare transient events. Detailed characterization of light propagation in the very local detector media throughout the instrumented volume will be critical for neutrino telescopes. Furthermore, increasing sampling of the Cherenkov radiation emitted by each event, made possible in a detector with more PMT instrumentation, will deliver significant improvements of angular resolution to current instruments. It is expected that next-generation telescopes will be able to reach a resolution of $\sim 0.2°$ at 1 PeV for muon tracks, and few-degree resolution for cascades, enabling more precise searches for multimessenger counterparts to astrophysical neutrinos (190, 191).

6.2. The Multimessenger Landscape in the Coming Decade

Understanding the physical processes at work in neutrino sources relies on the combined study of their neutrino and EM emission as a function of both time and energy. As neutrino telescopes

are wide-field instruments with nearly 4π sky coverage, these correlated studies require wide-field EM instruments, or pointed instruments that survey large swaths of the sky with high cadence. Prompt target-of-opportunity (ToO) observations, or long-term monitoring programs, of potential neutrino emitters may provide a similar temporal coverage over different timescales for a large collection of sources across the sky.

6.2.1. New instruments and expanded capabilities. High-energy extragalactic emitters such as AGNs that are potential neutrino sources display broadband emission features spanning the entire EM spectrum, from radio to VHE γ-rays. As discussed in Sections 4 and 5, EM tracers of hadronic emission may appear at different energy ranges depending on the properties of the source region, so their characterization requires broadband energy coverage. These observational campaigns, such as the one following the detection of IceCube-170922A and subsequent monitoring of TXS 0506+056 (67), are expected to continue in the coming years as more potential neutrino sources are identified, and they will be possible only if existing and upcoming EM facilities are in operation simultaneously. In the VHE ($E \gtrapprox 100$ GeV) γ-ray band, the upcoming Cherenkov Telescope Array (192, 193) will perform follow-up observations of neutrino alerts (194, 195), continuing the effort of current-generation instruments like H.E.S.S., MAGIC, and VERITAS (196) while also carrying out the most sensitive studies of extragalactic sources in the energy range between a few tens of GeV up to tens of TeV. These pointed observations will be supplemented by the monitoring capabilities of wide-field instruments currently in operation in the Northern Hemisphere, such as HAWC (197) and LHAASO (198), and the proposed SWGO in the Southern Hemisphere (199), where no such capability currently exists. For the foreseeable future, *Fermi*-LAT will remain the most sensitive instrument in the GeV band with all-sky coverage. A potential situation that should be avoided is an observational gap if *Fermi* stops operation before future missions, currently in their concept phase (e.g., 200), are launched.

As previously discussed, an important energy range for hadronic EM studies is the hard X-ray (>10 keV) to MeV band. For hard X-rays, *NuSTAR* (201) is the most sensitive telescope in operation while a gap exists in the MeV range, which is expected to be closed by upcoming missions in the next decade [e.g., *AMEGO* (202), *AMEGO-X* (203), *COSI* (204)]. For soft X-rays (<10 keV), the Neil Gehrels *Swift* observatory has been the main instrument for neutrino follow-up observations given its fast repointing capability (205), while *MAXI/GSC* (206) and *INTEGRAL* (207) offer larger sky coverage but with lower sensitivity. In this band, the *eROSITA* all-sky survey (208) will be key in providing a reference catalog against which flaring states of new or known extragalactic sources detected in neutrino ToO observations can be compared. Missions like *SVOM* (209) (to be launched in 2023) will also perform rapid neutrino follow-ups, while more sensitive telescopes like *Athena* will be used for detailed studies (210).

Correlation studies involving violent transients such as TDEs, GRBs, and supernovae with optical counterparts are already underway using observations from existing survey telescopes such as PanSTARRS (211), DES (212), and ZTF (213) and will be augmented in the coming years with the start of the LSST survey of the Vera C. Rubin Observatory (214). Wide multicolor optical surveys such as LSST and those conducted by space missions such as *Euclid* (215), *SPHEREx* (216), and the *Roman* space telescope (217) will also be critical to catalog other potential neutrino source classes such as star-forming galaxies (218). In the microwave range, future observatories such as CMB-S4 (219) can provide photometric coverage of extragalactic sources such as radio-loud AGNs and can enable correlated searches for transients, while in radio, upcoming facilities such as ngVLA (220) and ngEHT (221) can provide detailed, time-dependent imaging of the jet and core regions of potential sources such as AGNs.

GW detectors will also undergo important upgrades in the coming decade, starting with the addition of the KAGRA observatory to the existing LIGO and Virgo facilities (222) during their O4 run in 2022.

6.2.2. Interconnecting multimessenger facilities. As the neutrino emission may be due to transient or bursting/flaring extragalactic sources, it is critical that follow-up observations be performed shortly after a neutrino signal is identified. This requires that neutrino telescopes operate real-time searches that can isolate potential astrophysical signals, either as individual high-energy neutrinos or as spatial clusters of neutrino events over a given timescale, and it also requires a network over which these alerts can be broadcasted to the astronomical community for follow-up. IceCube sends out public real-time alerts for individual muon track and cascade events (singlets) of potential astrophysical origin, as well as private alerts to partner observatories for muon track multiplets over different timescales (58). Public alerts are communicated via the Gamma-ray Coordinates Network (GCN). ANTARES also operates singlet and doublet alert streams (57), and upcoming instruments such as KM3NeT (223) and Baikal-GVD (224) are already developing their real-time programs.

The large number of real-time streams becoming available for current and future multimessenger instruments has called for an upgrade of the communication infrastructure used to broadcast alerts, especially given the enormous alert rates expected for facilities such as the Rubin Observatory, which has an expected rate of 10 million alerts per night (225). Community alert brokers are currently under development to deliver this infrastructure for the Rubin Observatory, while other efforts such as Scalable Cyberinfrastructure to Support Multi-Messenger Astrophysics (SciMMA) (226) are more targeted toward the multimessenger community. GCN is expected to be superseded in the coming years by the Time-Domain Astronomy Coordination Hub (TACH) (227), while networks like the Astrophysical Multimessenger Observatory Network (AMON) (228, 229) are dedicated to real-time correlation studies of subthreshold streams from multimessenger observatories.

FUTURE ISSUES

1. Fully enabling extragalactic neutrino astronomy is within the reach of the next generation of high-energy neutrino telescopes.
2. The sensitivity of these studies will strongly rely on improvements in sensitivity and angular resolution.
3. Upcoming electromagnetic instruments will play a critical role in pinpointing multimessenger counterparts to neutrino signals and in characterizing their properties once sources are strongly detected. Joint GW-neutrino studies could also deliver multimessenger detections.
4. The interconnection of neutrino telescopes, both among themselves and with electromagnetic/GW facilities, will be key in identifying transient or bursting/flaring neutrino sources.
5. Further theoretical investigations, including numeric simulations on source dynamics and particle acceleration mechanisms, will be necessary to establish concordance pictures of multimessenger emission and to understand the physics of the neutrino sources.

DISCLOSURE STATEMENT

The authors are not aware of any affiliations, memberships, funding, or financial holdings that might be perceived as affecting the objectivity of this review.

ACKNOWLEDGMENTS

We thank Theo Glauch and Julia Tjus for useful comments. N.K. is supported by National Science Foundation (NSF) grant PHYS-1847827. The work of K.M. is supported by NSF grants AST-1908689, AST-2108466, and AST-2108467 and by KAKENHI grants 20H01901 and 20H05852. M.S. is supported by NSF grants PHY-1914579, PHY-1913607, PHY-1828168, PHY-2012944, OIA-2019597, and AST-2108517 and by NASA grants 80NSSC20K0049, 80NSSC20K0473, 80NSSC20K1494, and 80NSSC20K1587. In memory of Tom Gaisser, who was our kind mentor and a cornerstone of our field.

LITERATURE CITED

1. Davis R, Harmer DS, Hoffman KC. *Phys. Rev. Lett.* 20(21):1205 (1968)
2. Bahcall JN, Bahcall NA, Shaviv G. *Phys. Rev. Lett.* 20(21):1209 (1968)
3. Hirata K, et al. *Phys. Rev. Lett.* 58(14):1490 (1987)
4. Bionta RM, et al. *Phys. Rev. Lett.* 58(14):1494 (1987)
5. Aartsen M, et al. *Science* 342:1242856 (2013)
6. Haxton WC, Robertson RGH, Serenelli AM. *Annu. Rev. Astron. Astrophys.* 51:21 (2013)
7. Scholberg K. *Annu. Rev. Nucl. Part. Sci.* 62:81 (2012)
8. Tamborra I, Murase K. *Space Sci. Rev.* 214(1):31 (2018)
9. Markov MA. In *Proceedings of the 10th International Conference on High-Energy Physics (ICHEP 60)*, ed. ECG Sudarshan, JH Tinlot, AC Melissinos, pp. 578–81. Rochester, NY: Rochester Univ. (1960)
10. Reines F. *Annu. Rev. Nucl. Sci.* 10:1 (1960)
11. Greisen K. *Annu. Rev. Nucl. Sci.* 10:63 (1960)
12. Roberts A. *Rev. Mod. Phys.* 64(1):259 (1992)
13. Spiering C. *Eur. Phys. J. H* 37(3):515 (2012)
14. Ageron M, et al. *Nucl. Instrum. Meth. A* 656:11 (2011)
15. Adrián-Martínez S, et al. *J. Phys. G* 43(8):084001 (2016)
16. Sinopoulou A, Coniglione R, Muller R, Tzamariudaki E. *Proc. Sci.* ICRC2021:1134 (2021)
17. Abbasi R, et al. (IceCube Collab.) *Phys. Rev. D* 83:012001 (2011)
18. Avrorin AD, et al. arXiv:1908.05427 [astro-ph.HE] (2019)
19. Belolaptikov I, et al. *Proc. Sci.* ICRC2021:002 (2021)
20. Aartsen MG, et al. *J. Instrum.* 12(03):P03012 (2017)
21. Gaisser T, Halzen F. *Annu. Rev. Nucl. Part. Sci.* 64:101 (2014)
22. Abbasi R, et al. *Nucl. Instrum. Meth. Phys. Res. A* 700:188 (2013)
23. Abbasi R, et al. *Astropart. Phys.* 35:615 (2012)
24. Aartsen M, et al. *Phys. Rev. D* 99:032004 (2019)
25. Glashow SL. *Phys. Rev.* 118(1):316 (1960)
26. Chirkin D, Rhode W. arXiv:hep-ph/0407075 [hep-ph] (2004)
27. Learned JG, Mannheim K. *Annu. Rev. Nucl. Part. Sci.* 50:679 (2000)
28. Albert A, et al. *Eur. Phys. J. C* 78(12):1006 (2018)
29. Aartsen MG, et al. *Astrophys. J.* 886:12 (2019)
30. Albert A, et al. *Eur. Phys. J. C* 77:419 (2017)
31. Gaisser TK, Engel R, Resconi E. *Cosmic Rays and Particle Physics*. Cambridge, UK: Cambridge Univ. Press (2016)
32. Enberg R, Reno MH, Sarcevic I. *Phys. Rev. D* 78:043005 (2008)
33. Learned JG, Pakvasa S. *Astropart. Phys.* 3:267 (1995)

34. Aartsen MG, et al. *Phys. Rev. Lett.* 111:021103 (2013)
35. Gaisser TK, Jero K, Karle A, van Santen J. *Phys. Rev. D* 90(2):023009 (2014)
36. Drury LO. *Rep. Prog. Phys.* 46:973 (1983)
37. Abbasi R, et al. *Phys. Rev. D* 104(2):022002 (2021)
38. Abbasi R, et al. *Astrophys. J.* 928:50 (2022)
39. Aartsen MG, et al. *Phys. Rev. Lett.* 125(12):121104 (2020)
40. Ackermann M, et al. *Astrophys. J.* 799:86 (2015)
41. Murase K, Fukugita M. *Phys. Rev. D* 99(6):063012 (2019)
42. Murase K, Waxman E. *Phys. Rev. D* 94(10):103006 (2016)
43. Yoshida S, Murase K. *Phys. Rev. D* 102(8):083023 (2020)
44. Murase K, Ahlers M, Lacki BC. *Phys. Rev. D* 88(12):121301 (2013)
45. Ackermann M, et al. *Phys. Rev. Lett.* 116(15):151105 (2016)
46. Murase K, Guetta D, Ahlers M. *Phys. Rev. Lett.* 116(7):071101 (2016)
47. Capanema A, Esmaili A, Murase K. *Phys. Rev. D* 101(10):103012 (2020)
48. Capanema A, Esmaili A, Serpico PD. *J.Cosmol. Astropart. Phys.* 2102:037 (2021)
49. Aartsen MG, et al. *Astrophys. J.* 833(1):3 (2016)
50. Aartsen MG, et al. *Phys. Rev. D* 98(6):062003 (2018)
51. Aartsen MG, et al. *Phys. Rev. Lett.* 124(5):051103 (2020)
52. Albert A, et al. *Phys. Rev. D* 96(8):082001 (2017)
53. Albert A, et al. *Astrophys. J.* 892(2):92 (2020)
54. Abdollahi S, et al. *Astrophys. J. Suppl.* 247(1):33 (2020)
55. Ackermann M, et al. *Astrophys. J.* 810(1):14 (2015)
56. Wakely SP, Horan D. In *Proceedings of the 30th International Cosmic Ray Conference (ICRC 2007)*, Vol. 3, pp. 1341–44. Bonn, Ger.: Helmholtz Assoc. (2007)
57. Ageron M, et al. *Astropart. Phys.* 35(8):530 (2012)
58. Aartsen M, et al. *Astropart. Phys.* 92:30 (2017)
59. Dornic D, et al. *Proc. Sci.* ICRC2019:872 (2019)
60. Suvorova O, et al. *Proc. Sci.* ICRC2021:946 (2021)
61. Abbasi R, et al. *Astrophys. J.* 910(1):4 (2021)
62. Aartsen MG, et al. *Eur. Phys. J. C* 79(3):234 (2019)
63. Abbasi R, et al. *Astrophys. J.* 911(1):67 (2021)
64. Spiering C. arXiv:1903.11481 [astro-ph.HE] (2019)
65. Blaufuss E, Kintscher T, Lu L, Tung CF. *Proc. Sci.* ICRC2019:1021 (2020)
66. Kopper C, et al. *IceCube-170922A—IceCube observation of a high-energy neutrino candidate event*. GCN Circ. 21916, GRB Coord. Netw., NASA, Washington, DC (2017)
67. Aartsen MG, et al. *Science* 361(6398):eaat1378 (2018)
68. Aartsen M, et al. *Science* 361(6398):147 (2018)
69. Adrián-Martínez S, et al. *J. Cosmol. Astropart. Phys.* 1512:014 (2015)
70. Aartsen MG, et al. *Astrophys. J.* 835(1):45 (2017)
71. Hooper D, Linden T, Vieregg A. *J. Cosmol. Astropart. Phys.* 1902:012 (2019)
72. Smith D, Hooper D, Vieregg A. *J. Cosmol. Astropart. Phys.* 2103:031 (2021)
73. Albert A, et al. *Astrophys. J.* 911(1):48 (2021)
74. Abbasi R, et al. *Nature* 484:351 (2012)
75. Li Z. *Phys. Rev. D* 85:027301 (2012)
76. Hummer S, Baerwald P, Winter W. *Phys. Rev. Lett.* 108:231101 (2012)
77. He HN, et al. *Astrophys. J.* 752:29 (2012)
78. Adrián-Martínez S, et al. *Astron. Astrophys.* 559:A9 (2013)
79. Aartsen MG, et al. *Astrophys. J.* 805(1):L5 (2015)
80. Aartsen MG, et al. *Astrophys. J.* 824(2):115 (2016)
81. Adrián-Martínez S, et al. *Eur. Phys. J. C* 77(1):20 (2017)
82. Aartsen MG, et al. *Astrophys. J.* 843(2):112 (2017)
83. Albert A, et al. *Mon. Not. R. Astron. Soc.* 469(1):906 (2017)

84. Albert A, et al. *Mon. Not. R. Astron. Soc.* 500(4):5614 (2020)
85. Murase K, Bartos I. *Annu. Rev. Nucl. Part. Sci.* 69:477 (2019)
86. Aartsen MG, et al. *Astrophys. J.* 811(1):52 (2015)
87. Senno N, Murase K, Mészáros P. *J.Cosmol. Astropart. Phys.* 1801:025 (2018)
88. Esmaili A, Murase K. *J.Cosmol. Astropart. Phys.* 1812:008 (2018)
89. Necker J, et al. *Proc. Sci.* ICRC2021:1116 (2021)
90. Stein R, et al. *Nat. Astron.* 5(5):510 (2021)
91. Stein R. *Proc. Sci.* ICRC2019:1016 (2019)
92. Albert A, et al. *Astrophys. J.* 920(1):50 (2021)
93. Abbott BP, et al. *Astrophys. J.* 848(2):L12 (2017)
94. Albert A, et al. *Astrophys. J.* 850(2):L35 (2017)
95. Avrorin AD, et al. *JETP Lett.* 108(12):787 (2018)
96. Albert A, et al. *Eur. Phys. J. C* 77(12):911 (2017)
97. Albert A, et al. *Phys. Rev. D* 96(2):022005 (2017)
98. Adrián-Martínez S, et al. *Phys. Rev. D* 93(12):122010 (2016)
99. Albert A, et al. *Astrophys. J.* 870(2):134 (2019)
100. Aartsen MG, et al. *Astrophys. J.* 898(1):L10 (2020)
101. Abbasi R, et al. arXiv:2105.13160 [astro-ph.HE] (2021)
102. Albert A, et al. *Eur. Phys. J. C* 80(5):487 (2020)
103. Adrián-Martínez S, et al. *Astrophys. J.* 774(1):19 (2013)
104. Aartsen MG, et al. *Phys. Rev. Lett.* 117(24):241101 (2016). Erratum. *Phys. Rev. Lett.* 119(25):259902 (2017)
105. Mannheim K. *Astropart. Phys.* 3:295 (1995)
106. Aharonian FA. *New Astron.* 5:377 (2000)
107. Mucke A, Protheroe RJ. *Astropart. Phys.* 15:121 (2001)
108. Murase K. In *Neutrino Astronomy: Current Status, Future Prospects*, ed. T Gaisser, A Karle, pp. 15–31. Singapore: World Scientific (2017)
109. Padovani P, et al. *Mon. Not. R. Astron. Soc.* 484(1):L104 (2019)
110. Keivani A, et al. *Astrophys. J.* 864(1):84 (2018)
111. Ansoldi S, et al. *Astrophys. J. Lett.* 863:L10 (2018)
112. Gao S, Fedynitch A, Winter W, Pohl M. *Nat. Astron.* 3(1):88 (2019)
113. Cerruti M, et al. *Mon. Not. R. Astron. Soc.* 483(1):L12 (2019). Erratum. *Mon. Not. R. Astron. Soc.* 502:L21 (2021)
114. Gasparyan S, Bégué D, Sahakyan N. *Mon. Not. R. Astron. Soc.* 509(2):2102 (2021)
115. Murase K, Oikonomou F, Petropoulou M. *Astrophys. J.* 865(2):124 (2018)
116. Rodrigues X, et al. *Astrophys. J. Lett.* 874(2):L29 (2019)
117. Reimer A, Boettcher M, Buson S. *Astrophys. J.* 881(1):46 (2019). Erratum. *Astrophys. J.* 899:168 (2020)
118. Petropoulou M, et al. *Astrophys. J.* 891:115 (2020)
119. Zhang BT, Petropoulou M, Murase K, Oikonomou F. *Astrophys. J.* 889:118 (2020)
120. Xue R, et al. *Astrophys. J.* 886:23 (2019)
121. Kadler M, et al. *Nat. Phys.* 12(8):807 (2016)
122. Giommi P, et al. *Astron. Astrophys.* 640:L4 (2020)
123. Petropoulou M, et al. *Astrophys. J.* 899(2):113 (2020)
124. Rodrigues X, et al. *Astrophys. J.* 912(1):54 (2021)
125. Oikonomou F, et al. *J. Cosmol. Astropart. Phys.* 2110:082 (2021)
126. Berezinsky VS. In *Proceedings of the International Conference on Neutrino Physics and Astrophysics* "*Neutrino* '77", Vol. 1, p. 177. Moscow: Nauka (1977)
127. Eichler D. *Astrophys. J.* 232:106 (1979)
128. Protheroe RJ, Kazanas D. *Astrophys. J.* 265:620 (1983)
129. Stecker FW, Done C, Salamon MH, Sommers P. *Phys. Rev. Lett.* 66:2697 (1991)
130. Murase K, Kimura SS, Meszaros P. *Phys. Rev. Lett.* 125(1):011101 (2020)
131. Inoue Y, Khangulyan D, Doi A. *Astrophys. J. Lett.* 891(2):L33 (2020)
132. Anchordoqui LA, Krizmanic JF, Stecker FW. *Proc. Sci.* ICRC2021:993 (2021)

133. Kheirandish A, Murase K, Kimura SS. *Astrophys. J.* 922(1):45 (2021)
134. Bloom JS, et al. *Science* 333(6039):203 (2011)
135. Wang XY, Liu RY. *Phys. Rev. D* 93(8):083005 (2016)
136. Senno N, Murase K, Meszaros P. *Astrophys. J.* 838(1):3 (2017)
137. Dai L, Fang K. *Mon. Not. R. Astron. Soc.* 469(2):1354 (2017)
138. Lunardini C, Winter W. *Phys. Rev. D* 95(12):123001 (2017)
139. Murase K, et al. *Astrophys. J.* 902(2):108 (2020)
140. Hayasaki K. *Nat. Astron.* 5:436 (2021)
141. Reusch S, et al. arXiv:2111.09390 [astro-ph.HE] (2021)
142. Murase K, Thompson TA, Lacki BC, Beacom JF. *Phys. Rev. D* 84:043003 (2011)
143. Katz B, Sapir N, Waxman E. arXiv:1106.1898 [astro-ph.HE] (2011)
144. Murase K. *Phys. Rev. D* 97(8):081301 (2018)
145. Petropoulou M, et al. *Mon. Not. R. Astron. Soc.* 470(2):1881 (2017)
146. Waxman E, Bahcall JN. *Phys. Rev. Lett.* 78:2292 (1997)
147. Murase K, Nagataki S. *Phys. Rev. D* 73:063002 (2006)
148. Bahcall JN, Meszaros P. *Phys. Rev. Lett.* 85:1362 (2000)
149. Meszaros P, Rees MJ. *Astrophys. J. Lett.* 541:L5 (2000)
150. Murase K, Kashiyama K, Mészáros P. *Phys. Rev. Lett.* 111:131102 (2013)
151. Waxman E, Bahcall JN. *Astrophys. J.* 541:707 (2000)
152. Dai Z, Lu T. *Astrophys. J.* 551:249 (2001)
153. Dermer CD. *Astrophys. J.* 574:65 (2002)
154. Murase K, Nagataki S. *Phys. Rev. Lett.* 97:051101 (2006)
155. Guo G, Qian YZ, Wu MR. *Astrophys. J.* 890:83 (2020)
156. Murase K, Ioka K, Nagataki S, Nakamura T. *Astrophys. J.* 651:L5 (2006)
157. Gupta N, Zhang B. *Astropart. Phys.* 27:386 (2007)
158. Wang XY, Razzaque S, Mészáros P, Dai ZG. *Phys. Rev. D* 76:083009 (2007)
159. Murase K, Ioka K, Nagataki S, Nakamura T. *Phys. Rev. D* 78:023005 (2008)
160. Murase K, Ioka K. *Phys. Rev. Lett.* 111(12):121102 (2013)
161. Senno N, Murase K, Meszaros P. *Phys. Rev. D* 93(8):083003 (2016)
162. Tamborra I, Ando S. *Phys. Rev. D* 93(5):053010 (2016)
163. Grichener A, Soker N. *Mon. Not. R. Astron. Soc.* 507(2):1651 (2021)
164. Murase K, Mészáros P, Zhang B. *Phys. Rev. D* 79:103001 (2009)
165. Fang K, Kotera K, Murase K, Olinto AV. *Phys. Rev. D* 90(10):103005 (2014)
166. Carpio J, Murase K. *Phys. Rev. D* 101(12):123002 (2020)
167. Kimura SS, Murase K, Mészáros P, Kiuchi K. *Astrophys. J. Lett.* 848(1):L4 (2017)
168. Biehl D, Heinze J, Winter W. *Mon. Not. R. Astron. Soc.* 476(1):1191 (2018)
169. Ahlers M, Halser L. *Mon. Not. R. Astron. Soc.* 490(4):4935 (2019)
170. Kimura SS, et al. *Phys. Rev. D* 98(4):043020 (2018)
171. Fang K, Metzger BD. *Astrophys. J.* 849(2):153 (2017)
172. Decoene V, et al. *J. Cosmol. Astropart. Phys.* 2004:045 (2020)
173. Murase K, Inoue S, Nagataki S. *Astrophys. J. Lett.* 689:L105 (2008)
174. Kotera K, et al. *Astrophys. J.* 707:370 (2009)
175. Zandanel F, Tamborra I, Gabici S, Ando S. *Astron. Astrophys.* 578:A32 (2015)
176. Fang K, Olinto AV. *Astrophys. J.* 828(1):37 (2016)
177. Fang K, Murase K. *Nat. Phys.* 14(4):396 (2018)
178. Hussain S, et al. *Mon. Not. R. Astron. Soc.* 507(2):1762 (2021)
179. Loeb A, Waxman E. *J. Cosmol. Astropart. Phys.* 0605:003 (2006)
180. Thompson TA, Quataert E, Waxman E, Loeb A. arXiv:astro-ph/0608699 [astro-ph] (2006)
181. Tamborra I, Ando S, Murase K. *J.Cosmol. Astropart. Phys.* 1409:043 (2014)
182. Chang XC, Wang XY. *Astrophys. J.* 793(2):131 (2014)
183. Senno N, et al. *Astrophys. J.* 806(1):24 (2015)
184. Chakraborty S, Izaguirre I. *Phys. Lett. B* 745:35 (2015)

185. Roth MA, Krumholz MR, Crocker RM, Celli S. *Nature* 597(7876):341 (2021)
186. Blanco C, Linden T. arXiv:2104.03315 [astro-ph.HE] (2021)
187. Aartsen MG, et al. *J. Phys. G* 48(6):060501 (2021)
188. Agostini M, et al. *Nat. Astron.* 4(10):913 (2020)
189. Schumacher LJ, et al. *Proc. Sci.* ICRC2021:1185 (2021)
190. Aiello S, et al. *Astropart. Phys.* 111:100 (2019)
191. Abbasi R, et al. *Proc. Sci.* ICRC2021:1186 (2021)
192. Acharya BS, et al. *Astropart. Phys.* 43:3 (2013)
193. Gueta O. *Proc. Sci.* ICRC2021:885 (2022)
194. Acharya BS, et al. arXiv:1709.07997 [astro-ph.IM] (2018)
195. Sergijenko O, et al. *Proc. Sci.* ICRC2021:975 (2021)
196. Acciari VA, et al. *Proc. Sci.* ICRC2021:960 (2021)
197. Abeysekara AU, et al. *Astrophys. J.* 843(1):39 (2017)
198. Aharonian F, et al. *Chin. Phys. C* 45(2):025002 (2021)
199. Hinton J. *Proc. Sci.* ICRC2021:023 (2021)
200. Buckley JH, et al. *Proc. Sci.* ICRC2021:655 (2021)
201. Koglin J, et al. In *Proceedings of SPIE*, Vol. 7437: *Optics for EUV, X-Ray, and Gamma-Ray Astronomy IV*, ed. SL O'Dell, G Pareschi, Paper 74370C. Bellingham, WA: SPIE (2009)
202. Moiseev A, et al. *Proc. Sci.* ICRC2017:798 (2018)
203. Fleischhack H. *Proc. Sci.* ICRC2021:649 (2021)
204. Tomsick JA. *Proc. Sci.* ICRC2021:652 (2021)
205. Evans PA, et al. *Mon. Not. R. Astron. Soc.* 448(3):2210 (2015)
206. Kawamuro T, et al. *Astrophys. J. Suppl.* 238(2):32 (2018)
207. Ubertini P, Bazzano A. *Nucl. Instrum. Methods Phys. Res. A* 742:47 (2014)
208. Predehl P, et al. *Astron. Astrophys.* 647:A1 (2021)
209. Godet O, et al. *Proceedings of SPIE*, Vol. 8443: *Space Telescopes and Instrumentation 2012: Ultraviolet to Gamma Ray*, ed. T Takahashi, SS Murray, J-WA den Herder, Paper 84431O. Bellingham, WA: SPIE (2012)
210. Piro L, et al. arXiv:2110.15677 [astro-ph.HE] (2021)
211. Kankare E, et al. *Astron. Astrophys.* 626:A117 (2019)
212. Morgan R, et al. *Astrophys. J.* 883:125 (2019)
213. Rauch L. *EPJWeb Conf.* 207:03001 (2019)
214. Abell PA, et al. arXiv:0912.0201 [astro-ph.IM] (2009)
215. Laureijs R, et al. arXiv:1110.3193 [astro-ph.CO] (2011)
216. Doré O, et al. arXiv:1805.05489 [astro-ph.IM] (2018)
217. Doré O, et al. arXiv:1804.03628 [astro-ph.CO] (2018)
218. Lunardini C, Vance GS, Emig KL, Windhorst RA. *J. Cosmol. Astropart. Phys.* 1910:073 (2019)
219. Abazajian K, et al. arXiv:1907.04473 [astro-ph.IM] (2019)
220. Selina RJ, et al. *Proceedings of SPIE*, Vol. 10700: *Ground-Based and Airborne Telescopes VII*, ed. HK Marshall, J Spyromilio, Paper 107001O. Bellingham, WA: SPIE (2018)
221. Blackburn L, et al. arXiv:1909.01411 [astro-ph.IM] (2019)
222. Abbott BP, et al. *Living Rev. Rel.* 21(1):3 (2018)
223. Assal W, et al. *Proc. Sci.* ICRC2021:941 (2021)
224. Suvorova OV, et al. *Proc. Sci.* ICRC2021:946 (2021)
225. Bellm E, et al. *Plans and policies for LSST alert distribution*. Rep. LDM-612, Rubin Obs., Elqui Prov., Chile. (2019)
226. Brazier A, et al. In *American Astronomical Society Meeting Abstracts*, Vol. 235, Abstract 107.03. Washington, DC: Am. Astron. Soc. (2020)
227. Sambruna RM, et al. arXiv:2109.10841 [astro-ph.IM] (2021)
228. Smith MWE, et al. *Astropart. Phys.* 45:56 (2013)
229. Ayala Solares HA, et al. *Astropart. Phys.* 114:68 (2020)

Annual Review of Nuclear and Particle Science

Volume 72, 2022

Contents

Errata

An online log of corrections to *Annual Review of Nuclear and Particle Science* articles may be found at http://www.annualreviews.org/errata/nucl